AIIM

Association for Information and Image Management
1100 Wayne Avenue, Suite 1100
Silver Spring, Maryland 20910
301/587-8202

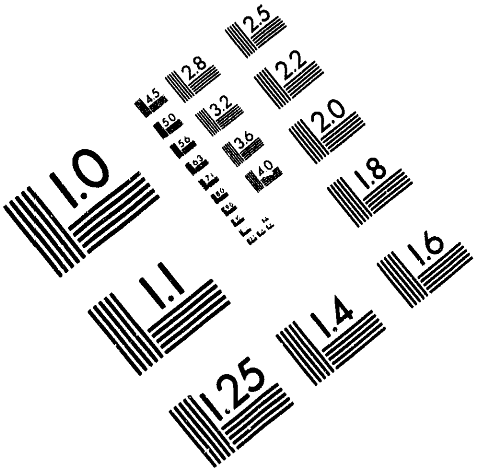
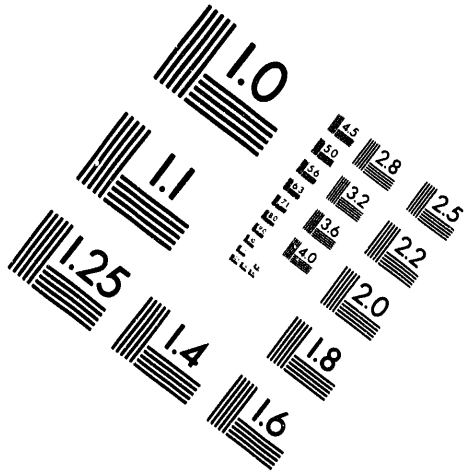

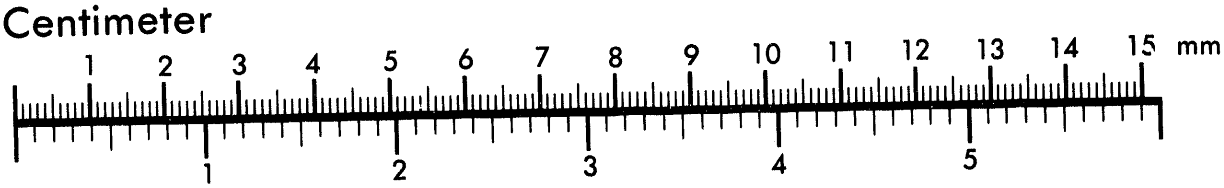

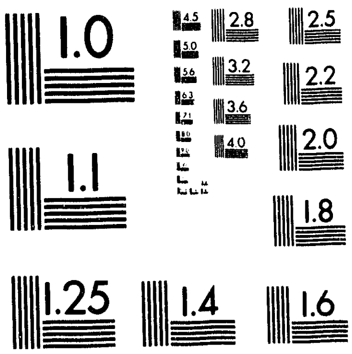

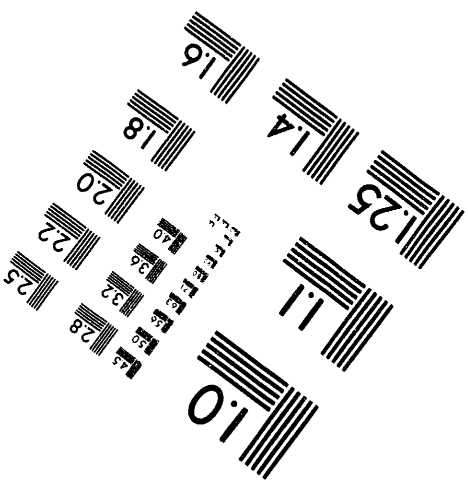
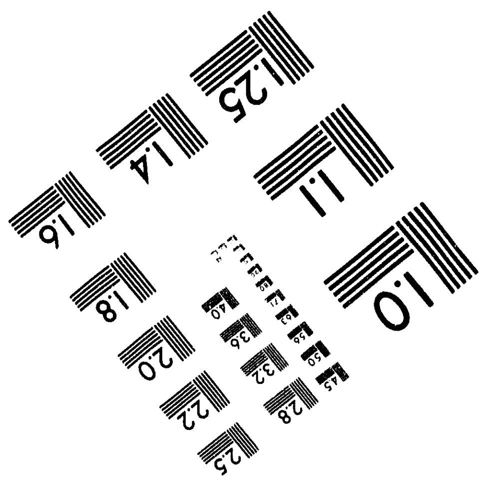

MANUFACTURED TO AIIM STANDARDS
BY APPLIED IMAGE, INC.

1 of 1

UCRL-JC-115106
PREPRINT

Adaptive Optics at Lick Observatory: System Architecture and Operations

J. M. Brase, J. An, K. Avicola, H. D. Bissinger, H. W. Friedman, D. T. Gavel, B. Johnston, C. E. Max, S. S. Olivier, R. Presta, D. A. Rapp, J. T. Salmon, K. E. Waltjen, W. Fisher

This paper was prepared for submittal to the
SPIE's 1994 Symposium on Astronomical Telescopes & Instrumentation
for the 21st Century
Kona, HI
March 13-18, 1994

March 1994

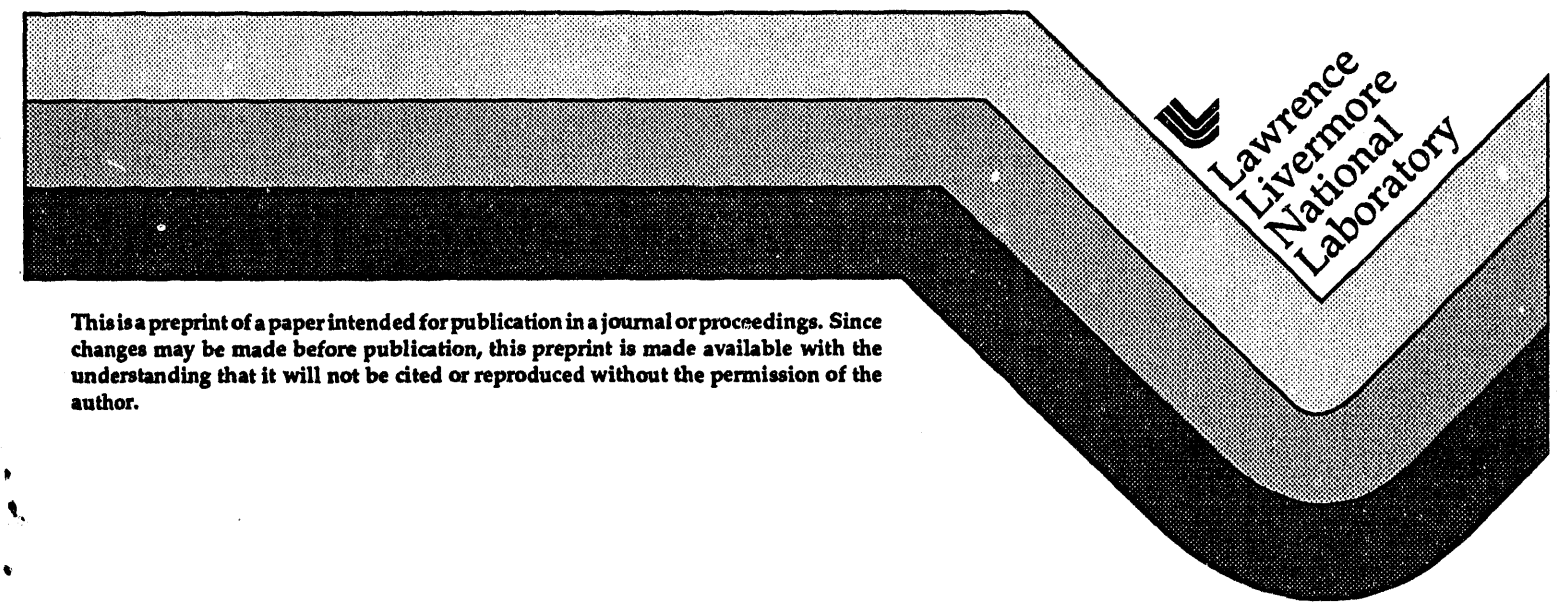

Adaptive optics at Lick Observatory: System architecture and operations

J.M. Brase, J. An, K. Avicola, H.D. Bissinger, H.W. Friedman, D.T. Gavel, B. Johnston, C.E. Max, S.S. Olivier, R. Presta, D.A. Rapp, J.T. Salmon, K.E. Waltjen

Lawrence Livermore National Laboratory
P.O. Box 808, L-495, Livermore, CA 94550

W. Fisher

Lockheed Palo Alto Research Laboratory
Palo Alto, CA 95304

Abstract

We will describe an adaptive optics system developed for the 1 meter Nickel and 3 meter Shane telescopes at Lick Observatory. Observing wavelengths will be in the visible for the 1 meter telescope and in the near IR on the 3 meter. The adaptive optics system design is based on a 69 actuator continuous surface deformable mirror and a Hartmann wavefront sensor equipped with an intensified CCD framing camera.

The system has been tested at the Cassegrain focus of the 1 meter telescope where the subaperture size is 12.5 cm. The wavefront control calculations are performed on a four processor single board computer controlled by a Unix-based system. We will describe the optical system and give details of the wavefront control system design. We will present predictions of the system performance and initial test results.

1. Introduction

Our objective is to develop an adaptive optics (AO) system for high-resolution astronomical imaging at the University of California's Lick Observatory on Mt. Hamilton. The general approach is to correct for atmospheric turbulence by measuring the wavefront from a known point source and then moving a deformable mirror surface to compensate. We are developing the system on the one meter Nickel reflector but the system is ultimately aimed at 1 - 2.2 μm imaging on the three meter Shane telescope. The system initially uses natural stars as reference sources but will use a sodium laser guide star when it becomes available [1].

In this paper, we will describe the design, implementation, and operation of the Lick AO system. We will develop some predictions of its performance an compare the results to initial laboratory tests and observatory experiments. A companion paper [2] describes in more detail the results of initial observations at Lick and plans for astronomical imaging.

2. The adaptive optics system design

2.1 System architecture

The architecture of the system is shown in Figure 1. In this section we will briefly go through the architecture and then describe each component in more detail. Light from the telescope enters the system from the Cassegrain focus as an F/17 beam. We first correct the overall tip-tilt error of the wavefront with a

piezoelectric controlled flat mirror. The beam is then collimated and sent to a deformable mirror (DM) at a plane conjugate to the telescope primary mirror. The DM has 69 actuators with a spacing (on the telescope pupil) of d = 12.5 cm. After reflection from the DM the light is split by a dichroic beam splitter. All light with wavelength shorter than 650 nm is sent to a wavefront sensor while the longer wavelength go on to the science camera. This wavelength cutoff point can be changed by substituting a selection of beamsplitters.

The wavefront sensor beam is then reformatted by an afocal telescope to the desired wavefront sensor aperture size. The wavefront sensor is a Shack-Hartmann system with a subaperture size matching the DM actuator spacing (d = 12.5 cm) capable of operating at up to 1000 frames per second. The wavefront sensor images are transferred to a wavefront control computer which reconstructs the error wavefront and generates the DM control signals at 1kHz.

After the dichroic beam splitter, the science camera beam is brought to an F/30 focus. The beam is again split by a 50% beam splitter. One beam goes to an avalanche photodiode quadcell which controls the tip-tilt mirror through an analog control system. The remaining beam goes to a thermo-electrically cooled Photometrics imaging camera with a detector scale of 0.047 arcsec/pixel.

The system is designed as a prototype for laser guide star (LGS) based correction. Since a LGS provides no overall tip-tilt information due to the atmospheric effects of the upgoing laser propagation [3], the tip-tilt must be corrected based on a natural guide star (NGS), the reason a separate sensor is used for tip-tilt rather than the wavefront sensor average tilt. For situations when a NGS is available for DM control, we will eventually provide a mode on which the tip-tilt mirror will be controlled by the wavefront sensor. We must also provide a refocusing capability for the wavefront sensor to switch from LGS to NGS operation. Another concern with LGS operation is the Rayleigh scattered light from the lower atmosphere. We will provide a field stop in the wavefront sensor afocal telescope to reject the scattered light. This issue is discussed in more detail in [1]. For the remainder of this paper we will assume a NGS reference for DM control since that is the mode we are currently operating.

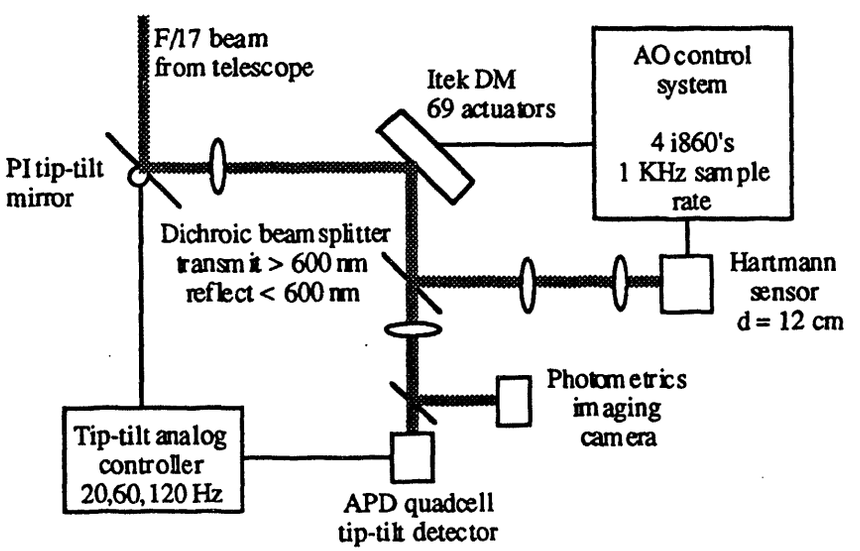

Figure 1. Block diagram of the Lick Observatory adaptive optics system

2.2 Wavefront sensor - intensified and bare CCD

The reference wavefront shape is measured with a Hartmann wavefront sensor[4]. An image of the telescope aperture is focused on an array of small lenslets which define the subapertures. Each lenslet focuses an image of the reference star on an imaging sensor. The centroid position of the images gives the average tip-tilt over the subaperture. These tilts can be reconstructed into the wavefront shape. The measurement must be repeated within the decorrelation time of the atmosphere, typically a few milliseconds.

For initial experiments, we are using an high speed Kodak camera coupled to the lenslet array by a two-stage image intensifier[5]. The lenslets form an 8x8 array of F/100 reference images. Each subaperture is a 10x10 array of 50 μm pixels with a detector scale of 1 arcsec/pixel. The Hartmann sensor images can be read from the camera at up to 2 KHz (but the controller can run at 1kHz maximum rate). The quantum efficiency of the intensifier-camera system is approximately 5%. The peak sensitivity of its S-20 phosphor is at 500 nm. The operation of this wavefront sensor is limited to reference stars with $m_v < 5$ on the 1 meter telescope by its low quantum efficiency.

The wavefront sensor is being upgraded to a bare-CCD camera using a Lincoln Laboratory developed CCD [6]. It is a 64x64 chip with QE η_{det}= 80% and read noise N_r = 10 e^-. at a 1 KHz frame rate. This wavefront sensor should increase the 1 meter limiting reference to $m_v = 7$.

The expected error in the wavefront measurement is described by the phase variance in the measurement. The error in calculating the centroid position for a Hartmann subaperture image is determined by the number of detected signal photons and the read noise of the sensor and is given by [15]

$$\sigma_{wfs} = \frac{6\pi^2}{16(SNR)}$$

where

$$SNR = \frac{\eta_{det} N_{phot}}{\sqrt{\eta_{det} N_{phot} + N_{pix} N_r^2}}$$

and Nphot is the number of reference photons per frame incident on a subaperture and Npix is the number of sensor pixels per subaperture. With N_{phot} = 1000 photons (mv = 4 for a 12 cm subaperture and 1 ms exposure) and $N_{pix} = 4$, the intensified camera SNR is 7 while the bare CCD camera SNR is 23 which gives σ_{wfs}(int) = 0.63 rad and σ_{wfs}(CCD) = 0.19 rad.

2.3 Deformable mirror

We are using an Itek continuous-face deformable mirror with 69 active actuators in a 9x9 square grid [7]. The PMN (lead - magnesium - niobate) actuators are separated by 7 mm on the mirror, equivalent to 12.5 cm on the telescope aperture. The actuators are placed at the corners of the wavefront sensor subapertures as shown in Figure 2. The lowest mechanical resonance of the mirror is > 5KHz, well above our 1 KHz maximum control system sample rate. The expected rms atmospheric wavefront fluctuations with tip-tilt removed are given by [8]

$$\sigma^2_{atmos} = 0.134\left(\frac{D}{r_0}\right)^{5/3}$$

which, for typical Lick conditions of r_0 = 8 cm and D = 1 meter, gives σ_{atmos} = 3.0 rad. For imaging at λ = 0.85 μm, allowing for $10\sigma_{atmos}$ errors requires an actuator stroke of at least 2 μm compared to the 3 μm stroke furnished by the mirror.

The deformable mirror can accurately represent spatial frequencies in the wavefront only up to a limit set by the actuator spacing. Higher spatial frequencies will contribute to the residual wavefront error. This error, generally called fitting error, has rms value [9] given by

$$\sigma_{fit}^2 = \kappa\left(\frac{d}{r_0}\right)^{5/3}$$

where d is the actuator spacing and κ is a constant which depends on the mirror influence function – the surface deflection due to moving a single actuator. If the subaperture size does not match the actuator spacing, the spatial sample interval d is the largest of the two. We will use $\kappa = 0.23$ for a Gaussian influence function, d = 12.5 cm for the Lick 1 meter telescope, and $r_0 = 8$ cm to give $\sigma_{fit} = 0.33$ rad.

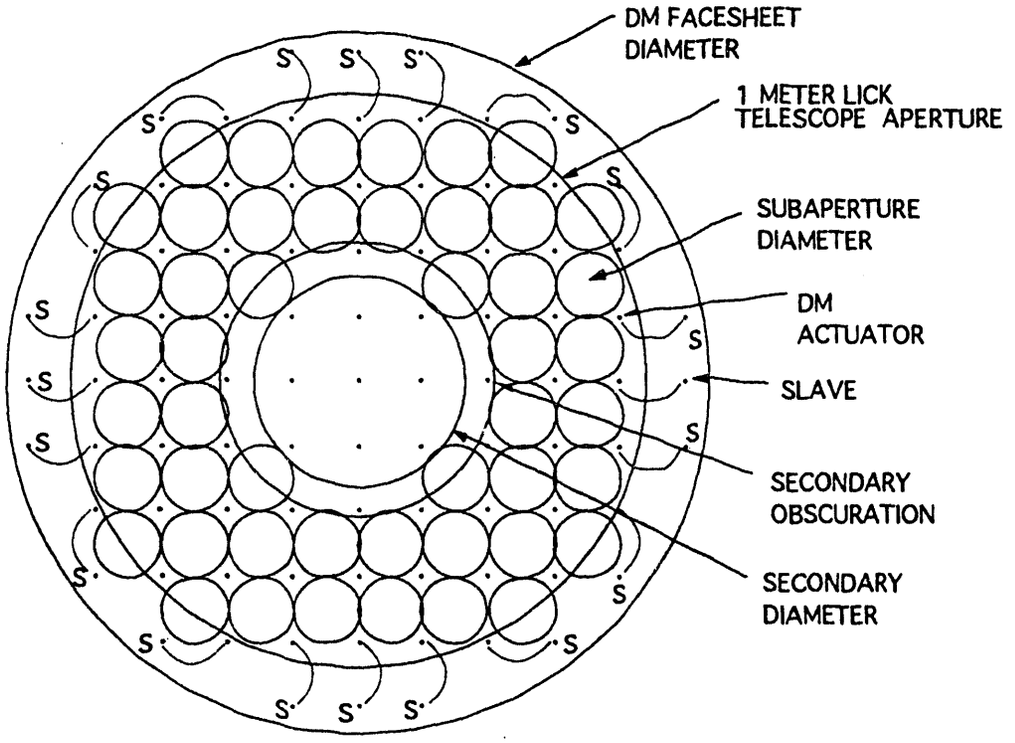

Figure 2. Deformable mirror and wavefront sensor geometry

2.4 Control system

The adaptive optics control system takes image data from the wavefront sensor and converts it to control signals for the deformable mirror. Its principal requirement is to minimize the delay between the measurement time and when the correction is sent to the deformable mirror relative to the atmospheric wavefront decorrelation time, typically a few milliseconds. The overall control process is shown in Figure 3. The measured slopes are reconstructed to give the error wavefront. This process gives the error at each actuator position in terms of the voltage signal to the actuator, essentially decoupling the 69 channels. It is followed by a standard PI controller for each actuator which determines the applied DM signal.

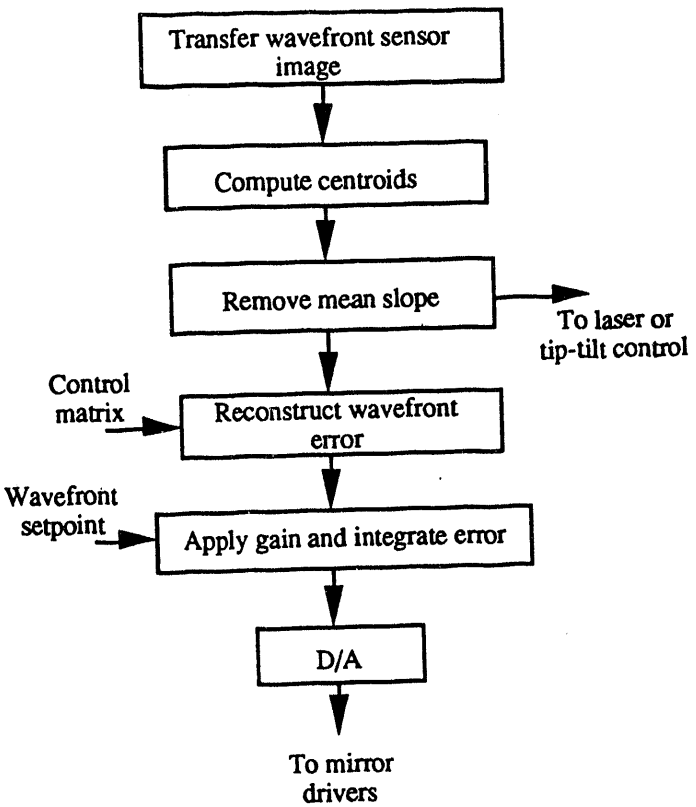

Figure 3. The wavefront control computational process

Our system is based on a Mercury single board parallel computer with four Intel i860 processors hosted by a Force Sparc-2 CPU running Unix. Its maximum sample rate is 1 KHz. It has two main computational tasks: computing Hartmann sensor image centroids to get wavefront slopes and doing a matrix-vector multiply to calculate the DM position commands from the slopes. A block diagram of the system hardware is shown in Figure 4.

Wavefront sensor image data is transferred into i860 shared memory at 50 Mbytes/sec. The overall real-time computational process is shown in the flowchart in Figure 3. For each subaperture, the system computes X and Y centroids and stores them in shared memory. The centroids are averaged to estimate the full-aperture tip-tilt which is then subtracted from the subaperture centroids. This full tip-tilt information will ultimately be used to control either the tip-tilt mirror for a NGS reference or the upgoing laser beam steering for a LGS reference.

To compute the required DM signals to correct the measured slope errors, we need to know the relationship between an applied actuator voltage and the observed wavefront sensor centroids. For a system with M subapertures and N actuators, we define the 2M component vector of slopes $\vec{\theta}$ and the N component actuator position vector $\vec{\varphi}$. They are related by 2MxN system matrix S such that $\vec{\theta} = S\vec{\varphi}$. We measure S by moving a single actuator through a series of voltages and recording the centroid positions. The slopes of the resulting response curves are a column of the system matrix S. This single matrix operation includes both the DM influence function and the gradient operation of the Hartmann sensor.

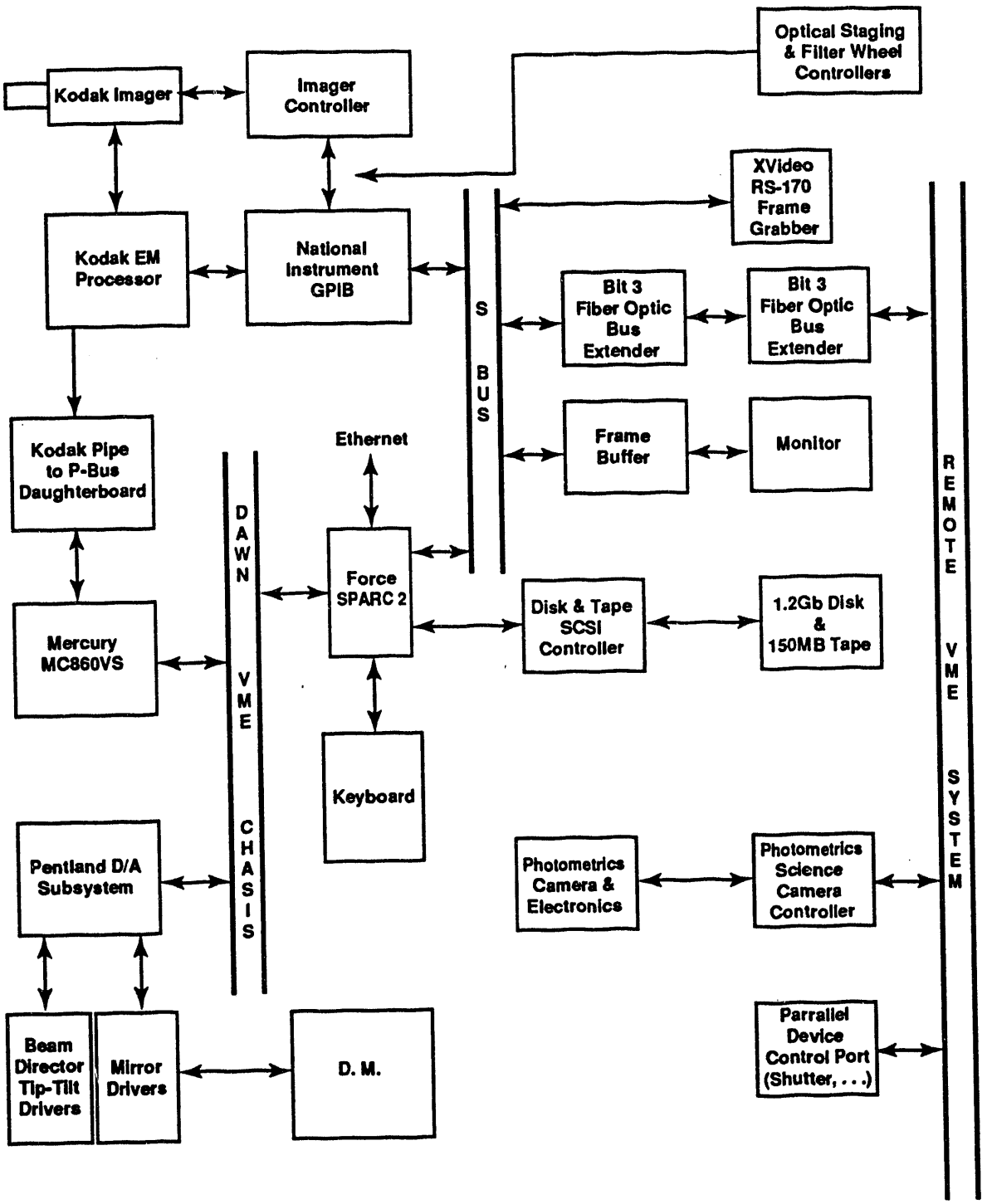

Figure 4. The adaptive optics electronic and computer hardware configuration

To compute the DM signals we apply the pseudoinverse of the system matrix to the slope measurements, $\vec{\varphi} = S^{+}\vec{\theta}$ [10]. We will refer to S^{+} as the control matrix. This matrix-vector multiply operation is the second major part of the real-time computational process shown in Figure 4. These signals are then multiplied by a control loop gain and integrated to form the actuator signals which are applied to the DM through a set of 69 parallel D/A converters.

For 1 KHz operation, the 1 msec camera integration period is followed by a 400 μsec data transfer to the computer. The centroid computation takes 300 μsec and the matrix-vector multiply and control calculations take 200 μsec. The average delay between sensing a wavefront change and applying a correction to the DM is 3 msec. The result of the delay is an inability to reject errors with temporal frequencies above a closed loop bandwidth of approximately $f_C = 30$ Hz. The controller performance is analyzed in more detail in a later section. The degradation in wavefront correction performance due to the delay is determined by the Greenwood frequency f_g [11],

$$\sigma^2_{control} = \left(\frac{f'_g}{f_c}\right)^{5/3}$$

where

$$f'_g = \frac{f_g}{1 + \frac{1}{\log(D/r_0)}}$$

is a correction to the Greenwood frequency that accounts for the fact that the atmosphere introduces less error at smaller D/r_0 even without any correction [15]. Choosing a nominal value for good conditions of $f_g = 80$ Hz, we expect $\sigma_{control} = 2.3$ rad, the largest error contributor of those we have discussed.

The wavefront setpoint of the controller is determined using a point source at the focal plane of the telescope. The DM is adjusted by addition of Zernuke modes to sharpen the image on the science camera [12]. When an optimum image is obtained the wavefront sensor image positions are recorded and used as the zero positions during atmospheric compensation. This technique allows correction of all static aberration in the system, even in the non-common path.

The system is controlled through a graphical user interface that allows interactive control of the parameters such as gain and integration. A slider control panel allows setting the controller setpoint to any combination of Zernike modes. The system furnishes diagnostic displays of time series or power spectra of centroids, reconstructed errors, and DM control signals.

2.5 Tip-tilt system

The tip-tilt system controls the overall position of the image on the science camera using a NGS reference. The image position is measured with a silicon avalanche photodiode quadcell which gives us a limiting magnitude (on the 1 meter telescope) of approximately $m_V = 7$. The mirror is controlled by an analog controller with selectable bandwidths of 20, 60, and 120 Hz. The system and described in detail in [13] and an analysis of the effects of tip-tilt errors is given in [14].

2.6 Optical system

The optical system layout is shown in Figures 5a and 5b for the front and rear of the optics table respectively. The system is mounted at the F/17 Cassegrain focus of Lick's Nickel reflector. The collimating and focusing elements are off-axis parabolas to reduce chromatic aberration since the system will use a guide star in the visible while imaging at wavelengths up to 2.2 μm.

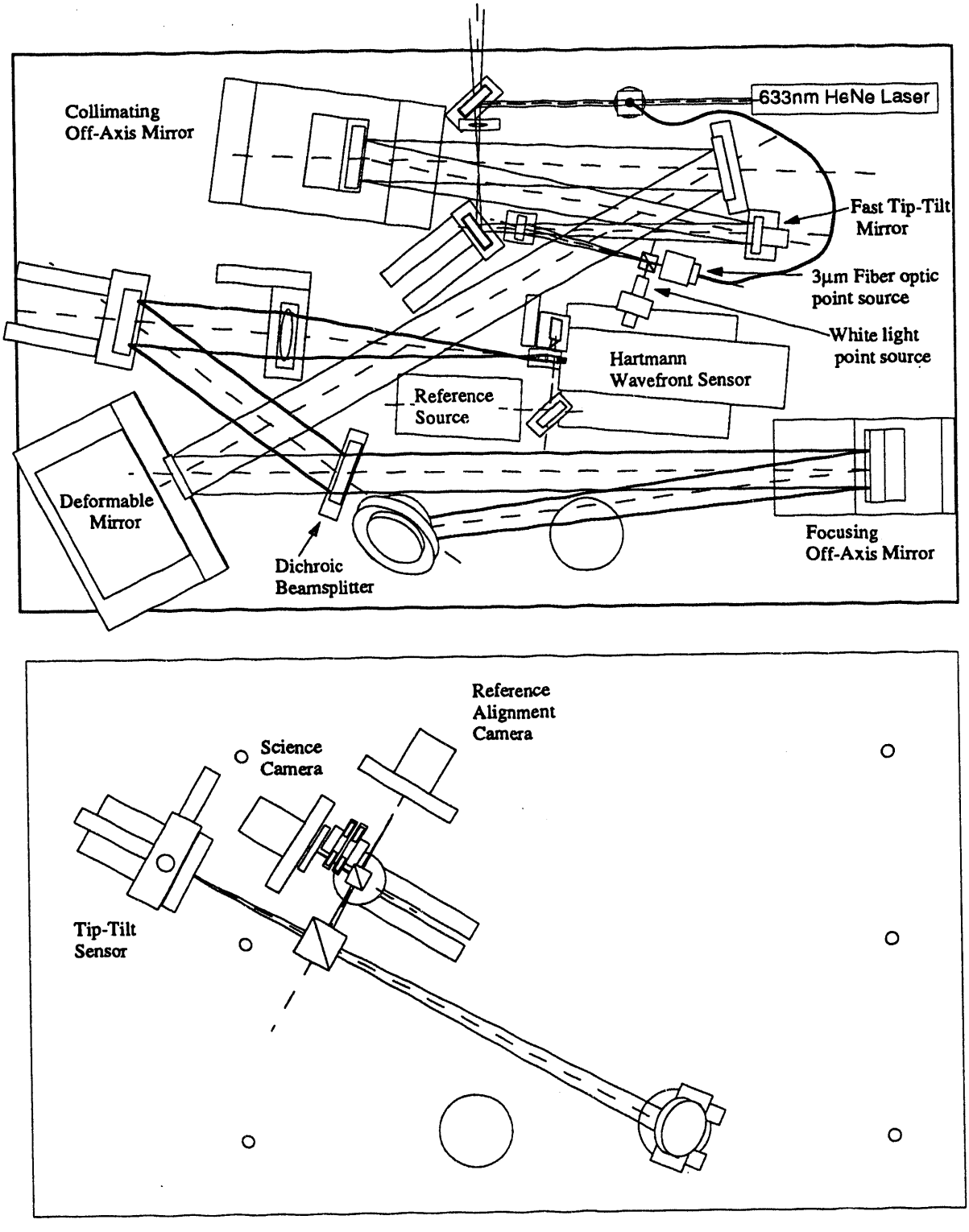

Figure 5. The front and back side optical layouts for the Lick Observatory adaptive optics system.

There are two internal reference sources in the optical system, both driven by a He-Ne laser. The first is for alignment and the second is a single-mode 3 μm fiber at the telescope focal plane which forms a diffraction-limited image for system calibration. An RS-170 video camera mounted in parallel with the science camera provides real-time alignment and diagnostic information.

3. System performance analysis

We will characterize the performance of the system by the Strehl ratio, the ratio of the peak image intensity to that of a diffraction-limited image. The Strehl is related to the wavefront variance by

$$S = e^{-\sigma_{wf}^2}$$

where σ_{wf}^2 is the sum of the wavefront error contributions discussed above

$$\sigma_{wf}^2 = \sigma_{wfs}^2 + \sigma_{fit}^2 + \sigma_{control}^2$$

We ignore for this analysis any errors due to anisoplanitism or imperfect tip-tilt correction. The details of this performance analysis process are fully described in [15].

The atmospheric conditions relevant to adaptive optics system performance for a single star correction are the spatial correlation length r_0 and the Greenwood frequency f_g, which have been defined above. At Lick Observatory r_0 and f_g vary over ranges from 3 to 10 cm and 40 to 200 Hz in poor to good seeing (all measurements at λ = 550 nm) [2]. We will define three sets of typical atmospheric conditions for Lick: poor seeing with r0 = 3 cm and fg = 200 Hz, average seeing with r0 = 5 cm and fg = 140 Hz, and good seeing with r0 = 10 cm and fg = 70 Hz.

In this section we will address two issues: the first is how the AO system performance scales the magnitude of the reference star, the second is the effect of the temporal bandwidth of the controller. These are currently the two main areas of development for the system. For the limiting magnitude issue, we will compare the two wavefront sensors described above for both the 1 and 3 meter telescopes and the set of atmospheric conditions described above. For the controller bandwidth issue, we will use the error model to look at general performance as the control loop bandwidth is varied.

3.1 System performance vs. NGS magnitude

One of the major issues in AO system performance is the limiting magnitude of the reference guide star. This determines sky coverage which, in turn, determines the objects that can be imaged. The limiting magnitude depends on the atmosphere and both the imaging and reference wavelengths. In this analysis we will fix the performance of the control loop and the DM to the nominal values described above and vary the atmospheric conditions. We will plot the system Strehl and discuss the improvement in Strehl over the uncorrected image where $S_{uncorr} = (D/r_0)^{-2}$ [15].

Figure 6 shows the intensified wavefront sensor system Strehl versus visual magnitude for good, average, and poor seeing as described above. In this case the NGS was a K type star (T_{eff} = 5000 deg. K). The uncorrected Strehls are 0.04, 0.009, and 0.003 respectively which give improvements of approximately 15, 13, and 5 for bright (mv = 0-3) stars. The improvements degrade rapidly as the star gets dimmer than mv = 4. The bright star results compares reasonably with preliminary observations in average seeing at Lick (see [2] for details) but the limiting magnitude predictions have not yet been tested.

To extend the system operation to dimmer reference stars, we are installing a bare CCD wavefront sensor as described above. Its performance versus NGS magnitude is compared to that of the intensified wavefront sensor in Figure 7. The performance shown is for average atmospheric conditions and an imaging

wavelength of 0.85 μm. The improved sensor will extend the limiting magnitude from approximately m_V = 5 to m_V = 7.

The tests that we are currently doing on the 1 meter telescope are aimed primarily at AO system development; the system is designed for astronomical imaging on the 3 meter telescope at 1 to 2.2 μm. In Figure 8 we show the system performance for good, average, and poor seeing on the 3 meter telescope at 1.6 μm (H band) with the bare CCD wavefront sensor. We have also assumed that we can increase the efficiency of the optical system from 15% to 40% and that we move the dichroic cutoff wavelength up to 1 μm. We should be able to use 10 - 12 magnitude stars under average to good seeing conditions. The system performance versus m_V is shown in Figure 9 for three wavelengths, 1.25 μm, 1.66 μm, and 2.2 μm.

3.2 System performance versus control system bandwidth

The most important error source in our current tests with bright stars is the wavefront error due to the delay in the control system. It is currently limiting us to approximately 30 Hz closed loop bandwidth. In this section we will look at the performance effects of increasing the bandwidth for both the current system on the 1 meter telescope with the intensified sensor and on the 3 meter system with the bare CCD sensor. In both cases we keep the sample rate fixed at 1KHz – the bandwidth is increased by reducing the system delay.

Figure 10 shows the Strehl performance of the 1 meter intensified wavefront sensor system for three different controller bandwidths, the current 30 Hz, 60 Hz, and 100Hz. With a sample rate of 1 KHz, 100 Hz is approximately the maximum achievable bandwidth with no additional delay in the controller. Figure 11 shows the same controller cases for the 3 meter telescope bare CCD wavefront sensor system (at 1.6 μm). For both systems we see that for bright reference objects, the increase in control bandwidth is very significant. As we go to dim sources where the error is dominated by the wavefront measurement, which will generally be the case for astronomical observations, the higher bandwidth may actually decrease the system performance because of lower effective averaging time in the controller [13]. The best course for the system design is probably to build in the highest possible bandwidth but allow the user to reduce the gain for dim objects.

4. Experimental results and conclusions

The adaptive optics system has been tested on the Lick 1 meter telescope on several nights over a period of four months. So far we have tested basic system operations by observing bright stars. These tests are described in more detail in [2]. Figure 12 shows an example image of α Aurigae at 850 nm; the open-loop image on the left, closed-loop on the right. The seeing during this experiment corresponded to the average case above and the Strehl improvement is approximately 10. The open and closed loop temporal slope spectra for the same case are shown in Figure 13. The controller has ~15 dB rejection of low frequencies and 30 Hz correction bandwidth.

We are actively working now to extend the system limiting magnitude by upgrading the wavefront sensor and moving to the 3 meter telescope where it will be equipped with a sodium laser guide star. The LGS-based adaptive optics system will open the entire sky to high resolution imaging in the 1 - 2.2 μm wavelength range.

5. Acknowledgements

This research was performed under the auspices of the U.S. Department of Energy, under contract number W-7405-ENG-48 to the Lawrence Livermore National Laboratory. The LLNL Laser Guide Star Project is supported by the LLNL Laboratory Directed Research and Development Program. Related work is supported by the Institute of Geophysics and Planetary Physics and by the Engineering Department at LLNL. We would like to thank the large group of LLNL technical staff who have provided support to the development of this system and to the staff of Lick Observatory for their support and assistance.

References

[1] H.W. Friedman, G. Erbert, T. Kuklo, J.T. Salmon, G. Smauley, G. Thompson, and N. Wong, "Design of a fieldable laser system for a sodium guide star", this conference, SPIE 2201 1994.

[2] S.S.Olivier, J. An, K. Avicola, H.D. Bissinger, J.M. Brase, H.W. Friedman, D.T. Gavel, E.M. Johansson, C.E. Max, K.E. Waltjen "Performance of adaptive optics at Lick Observatory", this conference, SPIE 2201, 1994.

[3] C.S. Gardner, B.M. Welsh, and L.A. Thompson, "Design and performance analysis of adaptive optical telescopes using laser guide stars", Proc. IEEE 78, 1721, 1990.

[4] R.K. Tyson, *Principles of Adaptive Optics*, Academic Press, 1991.

[5] K. Avicola, J.T.Salmon, J.M.Brase,K.Waltjen,R.Presta, and K.S.Balch"High framerate, large field wavefront sensor", in Proceedings of Laser Guide Star Adaptive Optics Workshop, R.Q.Fugate, ed. (U.S. Air Force Phillips Laboratory, Albuquerque, N.M., 1992).

[6] J. Twichell,B.E. Burke, R.K. Reich, W.H. McGonagle, C.M. Huang, M.W. Bautz, J.P. Doty, G.R. Ricker, R.W. Mountain, and V.S. Dolat, "Advanced CCD imager technology for use from 1 to 10000Å",Rev. Sci. Instrum. 61, 2744, 1990.

[7] M. Ealey and J. Washeba, "Continuous facesheet low voltage deformable mirrors", Optical Engineering 29, 10, 1191, 1990.

[8] R.J. Noll, "Zernike polynomials and atmospheric turbulence", J. Opt. Soc. Am. 66, 207, 1976.

[9] R. Hudgin, "Wavefront compensation error due to finite corrector-element size", J. Opt. Soc. Am. 67, 393, 1977.

[10] C. Boyer, V. Michau, G. Rousset, "Adaptive optics: Interaction matrix measurements and real time control algorithms for the COME-ON project", SPIE 1271, 63, 1990.

[11] D.P. Greenwood, "Bandwidth specification for adaptive optics systems", J. Opt. Soc. Am. 67, 390, 1977.

[12] A. Sarnik, "Phase retrieval: a practical application for the Space Telescope", SPIE 558, 85, 1985.

[13] K. Avicola, J.M. Brase, J. Morris, H.D. Bissinger, H. Friedman, D. Gavel, C. Max. S. Olivier, R. Kiefer, D. Rapp, J.T. Salmon, D. Smauley, K. Waltjen, "Sodium laser guide star system at Lawrence Livermore National Laboratory: system description and experimental results", this conference, SPIE 2201, 1994.

[14] S.S. Olivier and D.T. Gavel, "Tip-tilt compensation for astronomical imaging", J. Opt. Soc. Am. A 11, 368, 1994.

[15] S.S. Olivier, "Optimized performance of natural reference star adaptive optics systems", submitted to Ap. J., 1994.

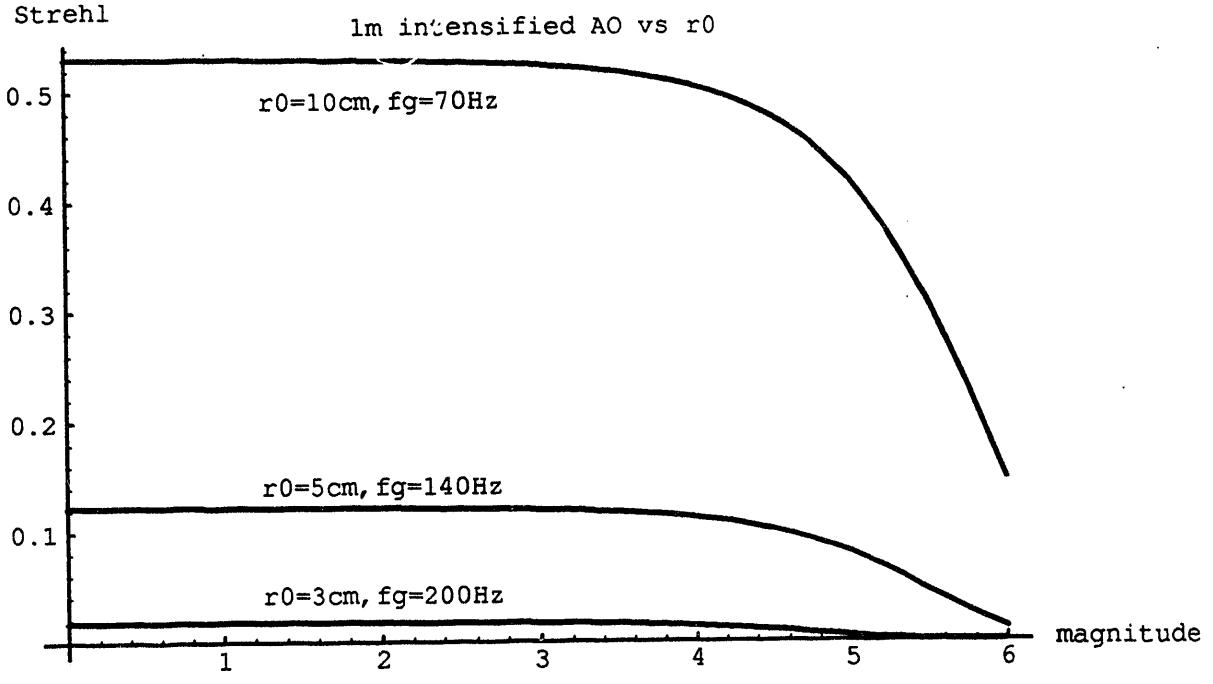

Figure 6. AO system performance versus reference star magnitude for good, average, and poor seeing at Lick Observatory using the intensified wavefront sensor system on the 1 meter telescope. The observing wavelength is 0.85 μm.

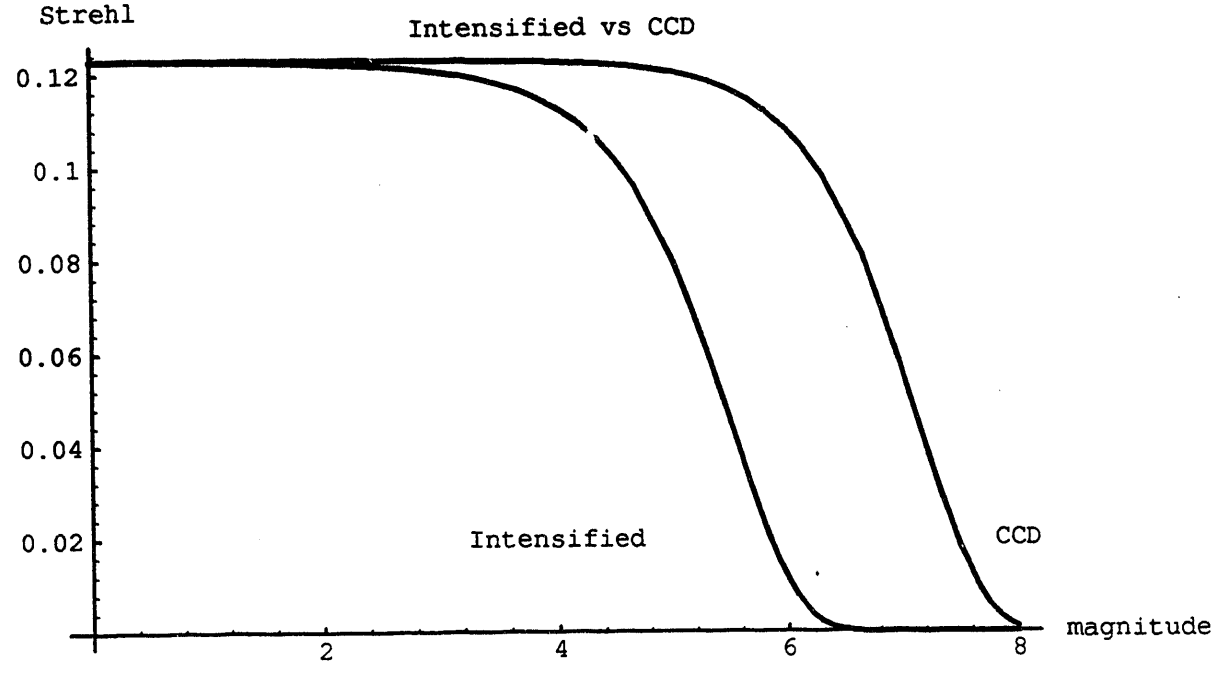

Figure 7. A comparison of AO system performance for the low QE intensified wavefront sensor versus the high QE, low-noise CCD based sensor.

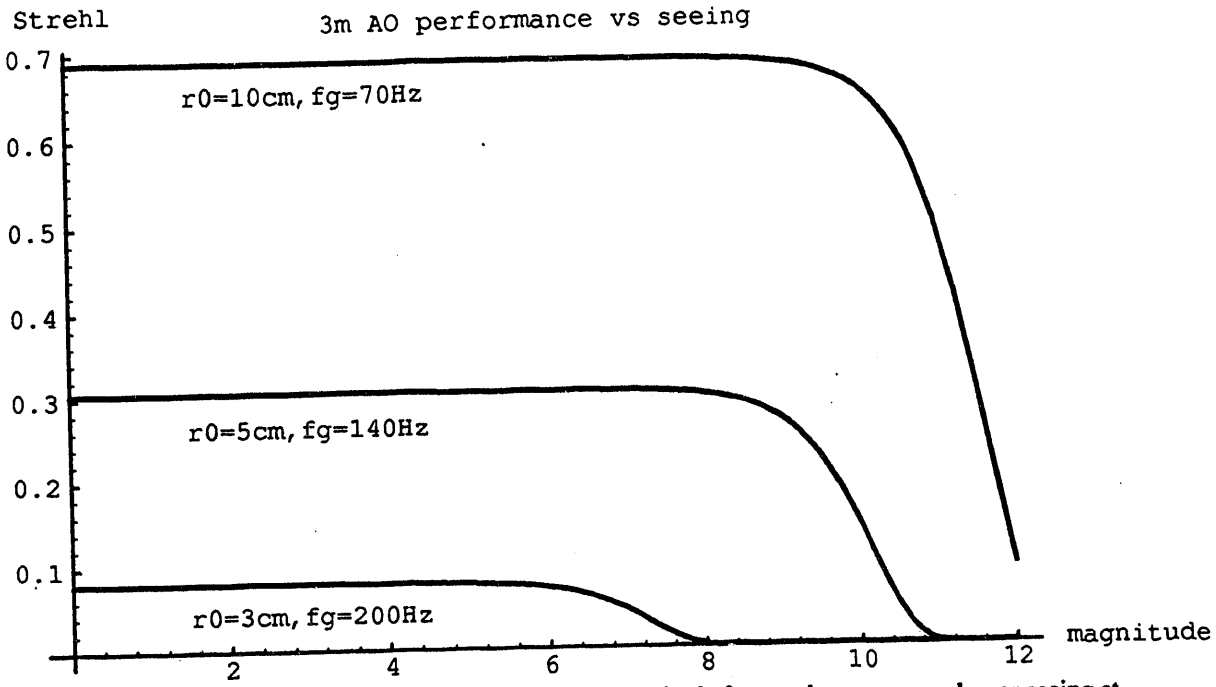

Figure 8. AO system performance versus reference star magnitude for good, average, and poor seeing at Lick Observatory using the bare CCD wavefront sensor system on the 3 meter telescope. The observing wavelength is 1.65 μm.

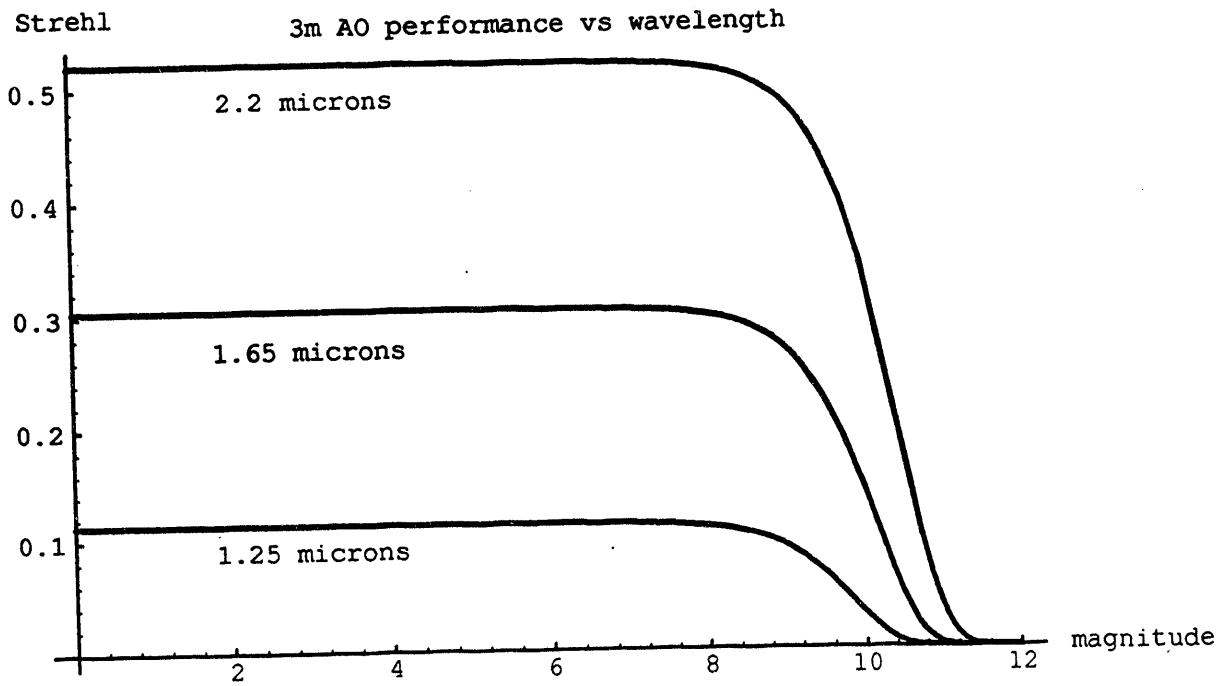

Figure 9. AO system performance versus reference star magnitude in good seeing for three wavelengths using the bare CCD wavefront sensor system on the 3 meter telescope.

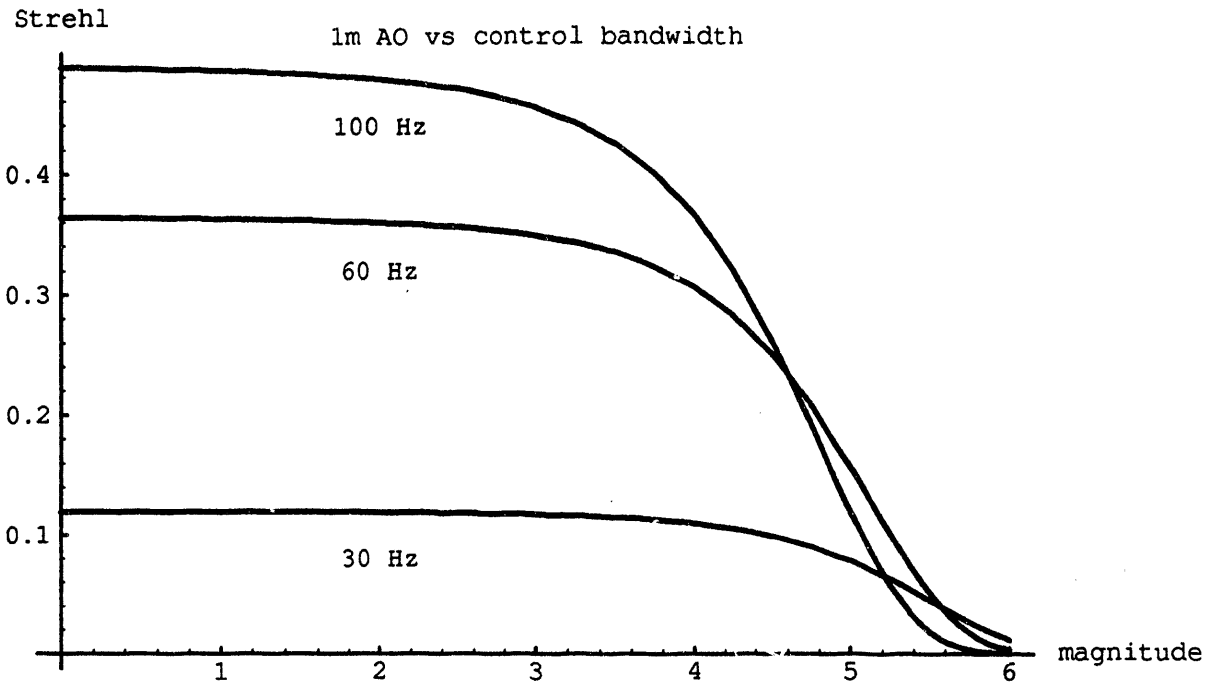

Figure 10. System performance versus reference star magnitude for three controller bandwidths on the 1 meter telescope with the intensified wavefront sensor. The observing wavelength is 0.85 μm.

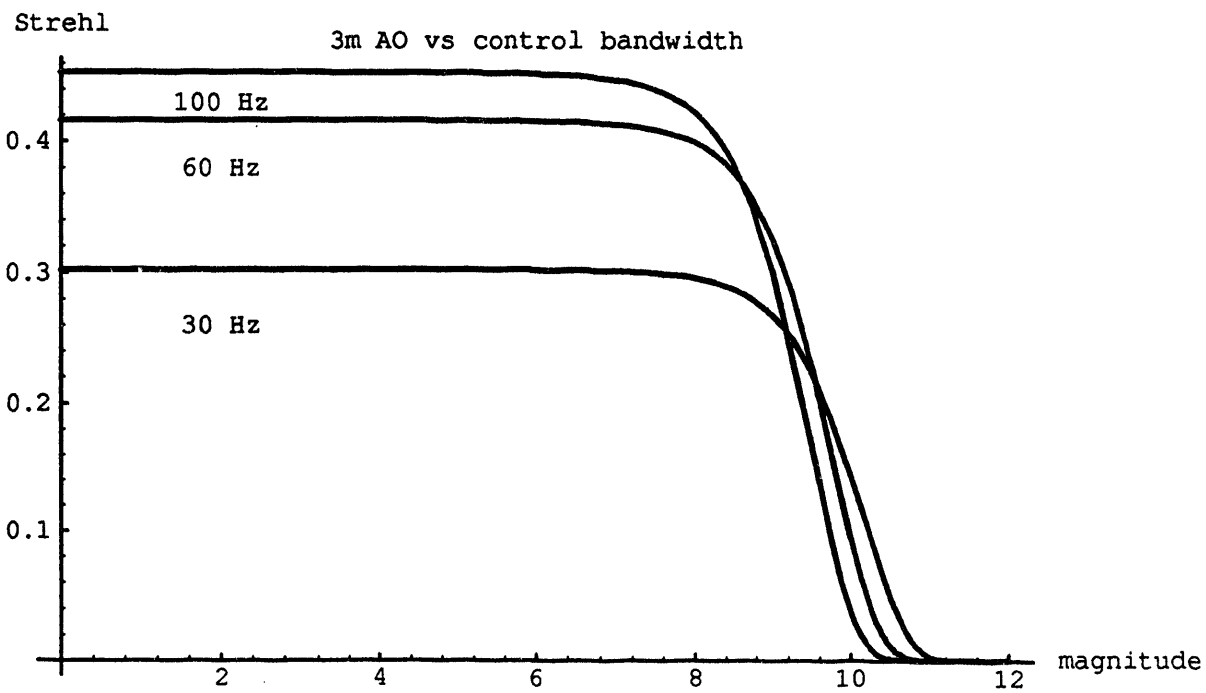

Figure 11. System performance versus reference star magnitude for three controller bandwidths on the 3 meter telescope with the bare CCD wavefront sensor. The observing wavelength is 1.65 μm.

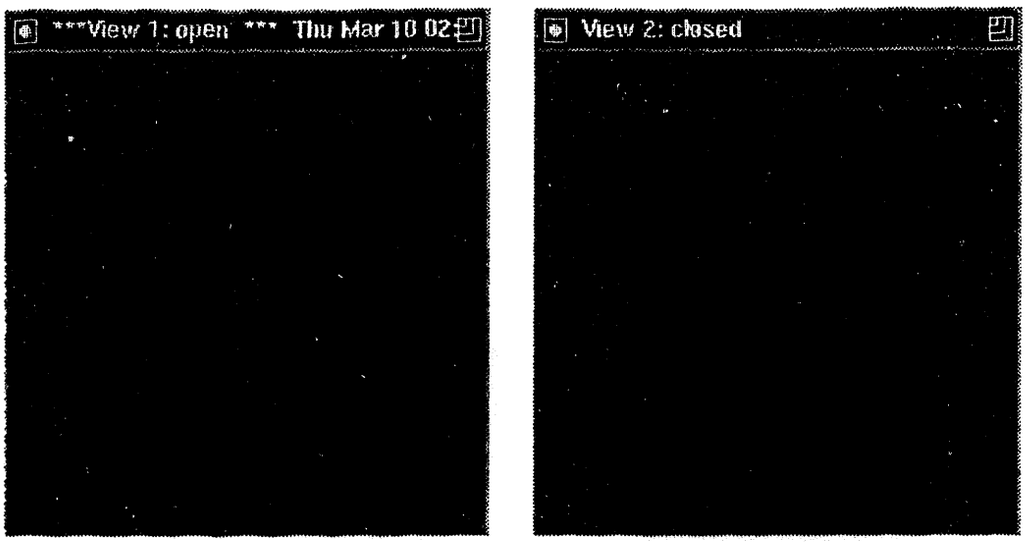

Figure 12. Open and closed loop images of alpha Aurigae at 850 nm. The open loop image is 2 arcsec FWHM, the closed loop image is 0.35 arcsec FWHM.

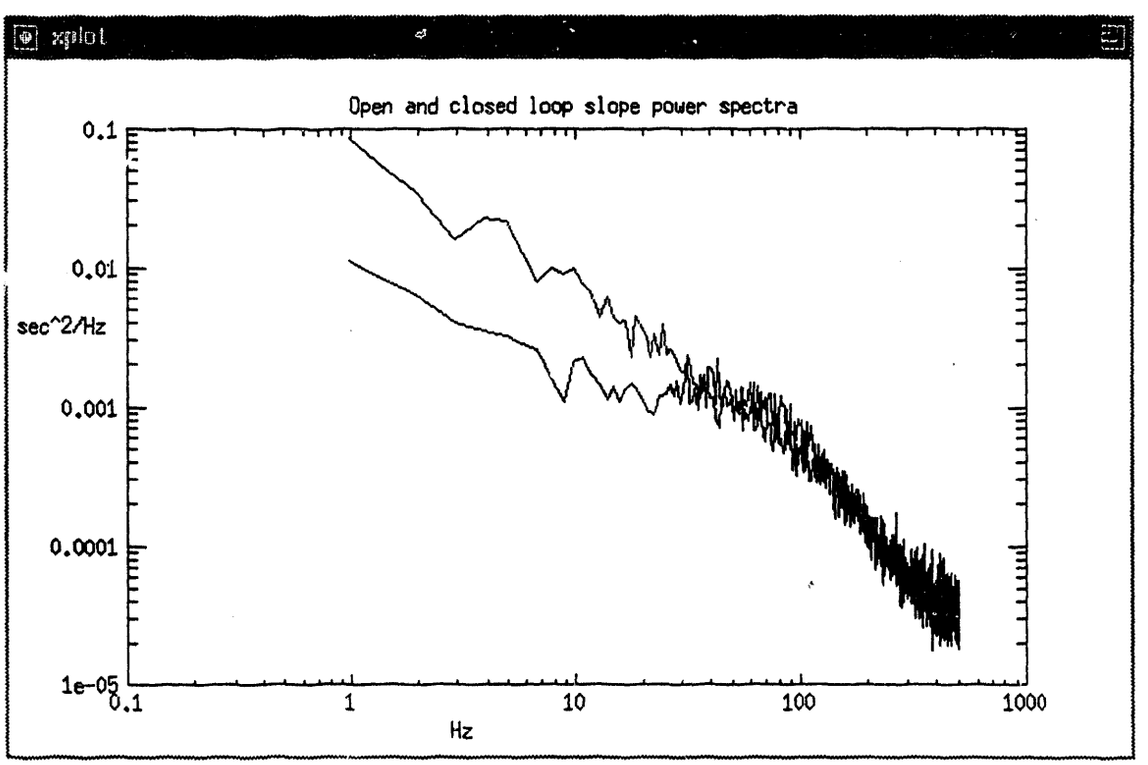

Figure 13. Open and closed loop slope power spectra for the above experiment.

DATE
FILMED
7/18/94

END